






Ultra-High-Performance C- and L-Band Radiometer System for Future Spaceborne Ocean Missions

Niels Skou , *Fellow, IEEE*, Sten Schmidl Søjbjerg, *Member, IEEE*, Steen Savstrup Kristensen , *Member, IEEE*, Cecilia Cappellin , *Member, IEEE*, Knud Pontoppidan, Jakob Rosenkrantz de Lasson, Marianna V. Ivashina , *Senior Member, IEEE*, and Oleg A. Iupikov , *Member, IEEE*

Abstract—A next-generation real-aperture spaceborne radiometer system for high-quality ocean measurements is discussed. Instead of illuminating the antenna reflector by a classical feed array of horn antennas in a one-feed-per-beam configuration, a multi-feed-per-beam configuration is chosen. Each antenna beam is thus created by adding the outputs from many small antenna elements in the feed array, thus providing an antenna beam of unsurpassed quality. This solves the classical polarization purity and land/sea contamination issues. The concept requires many microwave receivers and fast analog-to-digital converters as well as fast digital signal processing onboard the satellite. This is discussed, and resource budgets, especially concerning power, are provided.

Index Terms—Focal plane array (FPA), microwave, radiometer, receiver.

I. INTRODUCTION

FUTURE generations of spaceborne microwave radiometer missions, measuring the sea surface temperature (SST) and the wind vector, will require a very good radiometric sensitivity around 0.25 K for the full Stokes vector and at the same time a good spatial resolution approaching 20 km at C- and X-bands and 10 km at Ku-band [1], [2].

For a typical 800 km orbit and 53° incidence angle, the footprint (FP) requirement calls for reflector antennas with 5 m aperture.

The performance requirements represent a significant improvement compared with existing spaceborne radiometer systems, such as AMSR-E [3] and WindSat [4]. They feature spatial resolutions around 55, 35, and 20 km at C-, X-, and Ku-bands, respectively, and the radiometric sensitivity provided by AMSR-E is 0.3 K at C-band and 0.6 K at X- and Ku-bands, while for WindSat it is around 0.7 K.

Manuscript received July 10, 2018; revised December 14, 2018; accepted January 10, 2019. Date of publication February 22, 2019; date of current version July 17, 2019. This work was supported by the European Space Agency through contracts with ESTEC (4000107369/12/NL/MH and 4000117841/16/NL/FF/gp) and Airbus (ASE-B-18-767) and by the Swedish National Space Board (202/15). (Corresponding author: Niels Skou.)

N. Skou, S. S. Søjbjerg, and S. S. Kristensen are with the DTU Space, Technical University of Denmark, Kongens Lyngby 2800, Denmark (e-mail: ns@space.dtu.dk; sss@space.dtu.dk; ssk@space.dtu.dk).

C. Cappellin, K. Pontoppidan, and J. R. de Lasson are with TICRA, Copenhagen, Denmark. (e-mail: cc@ticra.com; kp@ticra.com; jrdl@ticra.com).

M. V. Ivashina and O. A. Iupikov are with the Chalmers University of Technology, Gothenburg 41296, Sweden (e-mail: marianna.ivashina@chalmers.se; oleg.iupikov@chalmers.se).

Color versions of one or more of the figures in this paper are available online at <http://ieeexplore.ieee.org>.

Digital Object Identifier 10.1109/JSTARS.2019.2894846

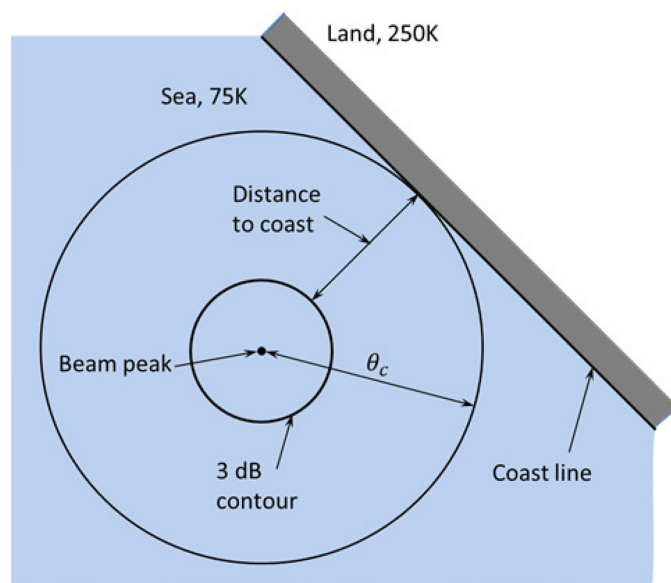


Fig. 1. Schematic of the distance to coast issue.

An important requirement concerns the cross polarization of the antenna. The radiometer shall measure brightness temperatures in two linear polarizations, vertical and horizontal, and with an accuracy of 0.25 K. This requires that the cross-polar power received from the Earth does not exceed 0.34% of the total power coming from the Earth for that polarization state [5]. This represents a severe antenna requirement, and it is difficult to design a reflector antenna with a traditional feed horn or cluster of horns that fulfills this challenge. A focal plane array (FPA) of densely spaced active antenna elements that is used as feed can overcome these problems, as we shall see later.

Another very challenging requirement is that the instrument must be able to measure ocean parameters correctly as close as 5–15 km from the coast. Assuming a brightness temperature of the sea between 75 and 150 K for H and V polarizations, and of the land 250 K, the required accuracy of 0.25 K is obtained if the coastline is located outside a cone, around the main beam and with angle θ_c , containing 99.7% of the total power on the Earth [5]. In order to obtain a small distance to coast, this cone must be as narrow as possible (see Fig. 1). The 5–15 km requirement represents a major improvement as current systems feature about 100 km distance to coast capability (the so-called land/sea contamination issue). Meeting this requirement is

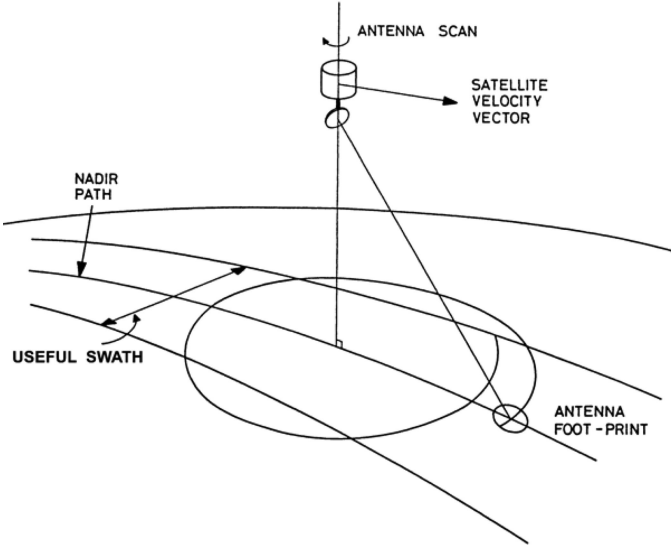


Fig. 2. Schematic of scanning radiometer system.

practically impossible with a reflector and a traditional feed horn, while an FPA as feed can do the job.

It should also be noted that minimizing the cone angle θ_c can be viewed as minimizing the side lobes of the antenna radiation pattern.

For all three frequency bands, the bandwidths are limited to a few hundreds of megahertz, and hence, even the most optimistic receiver noise properties cannot ensure the required radiometric sensitivity when considering a single-beam scanning system. For a scanner, as shown in Fig. 2, the only solution is to employ several independent antenna beams per frequency and to improve sensitivity by integration of several FPs. This calls for a host of feeds/beams and associated receivers—could be 10 or more beams at Ku-band. The scanner will typically cover a swath of ≈ 1500 km.

II. ANALYSIS OF TYPICAL SCANNER

In the following, relations between the antenna aperture (D), the FP, the integration time (τ), the radiometric resolution (ΔT), the antenna rotation rate (RPM), and the number of beams for a typical scanner will be worked through. In addition to C-, X-, and Ku-bands, L- and Ka-bands are also considered as they are traditional and important frequency bands.

A. Instrument Specifications and Requirements

To make the deliberations more concrete the following realistic assumptions for a new, advanced mission are made:

- 1) altitude = 817 km;
- 2) incidence angle = 53° ;
- 3) swath = >1400 km;
- 4) TA = 150 K;
- 5) The FP is the intersection between a plane Earth surface and the antenna beam at -3 dB level. The value for the FP is the arithmetic mean of the FP along track (FPL) and across track (FPS).

TABLE I
SPECIFICATIONS AND REQUIREMENTS

Frequency (GHz)	1.4	6.925	10.65	18.7	36.5
Bandwidth (MHz)	19	300	100	200	300
FP (km) req.	?	20	15	10	5
ΔT (K) req.	0.15	0.15	0.3	0.3	0.3

TABLE II
NOISE FIGURE AND NOISE TEMPERATURE

Frequency	Pre-amp NF (dB)	Switch loss (dB)	Line loss (dB)	Total (dB)	T_N (K)
L	0.4	0.4	0.2	1.0	76
C	0.6	0.5	0.3	1.4	110
X	1.2	0.6	0.3	2.1	180
Ku	1.5	0.7	0.4	2.6	238
Ka	1.5	1.0	0.5	3.0	290

- 6) 30% FP overlap is required both across track and along track to avoid aliasing in the sampling process.
- 7) Channel specifications and requirements are shown in Table I.

The L-band channel is to be regarded as optional. Hence, it cannot drive the design, especially concerning the antenna size.

B. Analysis of a Baseline Scanner

A conically scanning system is evaluated concerning the antenna size, the spatial resolution, the radiometric resolution, the coverage, and the antenna rotation rate assuming one single antenna beam.

For this, the method, as described in [6], is used. A circular antenna electrical aperture (D) and classical, circular feed horns are assumed. During the Advanced Radiometer Study [2], careful modeling confirmed that spatial resolution found this way is realistic also when FPAs in the end are used. The scanning antenna is rotating around a vertical axis, and the boresight direction, where the FP centers will be located, traces out a circle on the ground. The “useful” swath can be reasonably defined by using $\pm 60^\circ$ of the potentially $\pm 90^\circ$ scan angle. Beyond 60° , the increase in the effective swath is quite limited. Only forward looking is assumed. This does not preclude utilizing both fore-and-aft looking at later stages if the spacecraft layout permits this. Calibration is assumed to take place while the scanner looks away from the $\pm 60^\circ$ swath. If fore-and-aft looking is used, the $\pm 60^\circ$ definition leaves enough time available for internal calibration—or space available for external targets.

For the 817 km altitude and 53° incidence angle, the “useful” swath becomes 1524 km.

In [6], assumptions about the receiver bandwidth and noise figures are made in order to carry out a general discussion. Here, actual bandwidths and current estimates of state-of-the-art noise performances are used. State-of-the-art total power receivers are assumed. Table II shows receiver noise issues assuming a

TABLE III
C-BAND FP, ANTENNA ROTATION RATE (RPM), AND
RADIOMETRIC RESOLUTION (ΔT)

D (m)	FPS (km)	FPL (km)	FP (km)	τ (msec)	RPM	ΔT (K)
3	25.1	41.7	33.4	14.0	13.6	0.13
4	18.8	31.3	25.1	7.9	18.1	0.17
5	15.1	25.0	20.1	5.1	22.6	0.21
6	12.6	20.9	16.7	3.5	27.2	0.25
7	10.8	17.9	14.3	2.6	31.7	0.30

classical receiver design with a low-noise pre-amplifier preceded by a calibration switch.

Low-loss antenna feed elements are assumed, with the very small (MMIC) receivers mounted directly on the feed element ports.

The antenna is assumed to look at a calm sea surface at V polarization. Hence, the brightness temperatures can be calculated using the method by Klein & Swift [7]. However, for simplicity, just one common value $T_A = 150$ K is used here for all frequencies.

C-band is an important channel for an ocean mission, so we will start with that frequency. Results for a scanner having antenna apertures in the range 3–7 m are shown in Table III.

It is seen that a 5-m aperture leads to elongated FPs (15 by 25 km) with an arithmetic mean equal to the required 20 km. So, the antenna size is now fixed to a 5 m aperture.

ΔT will be around 0.21 K, and the antenna will rotate with 22.6 RPM. The radiometric sensitivity is not satisfactory, and the rotation rate will, for mechanical and momentum compensation reasons, be very challenging for such a large reflector. We can implement several beams along track in order to lower the antenna rotation rate. Lower rotation rate leads to longer integration time and, hence, better sensitivity. Two beams along track and 2 associated receiver systems will improve the sensitivity by $\sqrt{2}$, resulting in $\Delta T = 0.15$ K, and reduce the rotation rate to 11.3 RPM. For comparison, NASA's Soil Moisture Active Passive (SMAP) instrument [8] with its 6 m mesh antenna rotates with 15 RPM, so this is deemed satisfactory from a mechanical point of view. Also, the radiometric resolution is now within requirements.

The contents of Table III for C-band can be worked out for all other frequencies. This has been done, but all tables are not shown here—only relevant results are quoted.

An X-band channel will have an FP of 13 km, $\Delta T = 0.71$ K, and 35 RPM rotation rate.

In order to fit the antenna rotation already determined by C-band issues, we must have three beams along track, resulting in $\Delta T = 0.41$ K. This is not satisfactory, so we must add extra beams across track. If we, for all three beams along track, add an additional across track beam, i.e., six beams in total, we achieve a $\Delta T = 0.29$ K, which is compliant with the requirements.

The FP is seen to become slightly smaller than required, which is probably quite acceptable.

The Ku-band channel will have an FP of 7.4 km, $\Delta T = 1.04$ K, and 61 RPM rotation. Again the FP is slightly smaller than required.

Five beams along track will ensure almost correct coverage and result in $\Delta T = 0.47$ K. Strictly speaking, five beams cannot cover the ground with the required 30% FP overlap but will provide 25% overlap. This is most probably acceptable, bearing in mind the cost of having one extra along-track beam. Additional beams across track are needed to achieve the required ΔT . Another row of beams, i.e., $5 \times 2 = 10$ beams, will result in $\Delta T = 0.33$ K, which is probably acceptable.

The Ka-band channel will have an FP of 3.8 km, $\Delta T = 1.88$ K, and 119 RPM rotation.

We need 10 beams along track for the correct coverage, and this will result in $\Delta T = 0.59$ K. The radiometric resolution is still far from acceptable, and one additional row of beams leads to $\Delta T = 0.42$ K, which is still not satisfactory. If we add yet another row of beams, i.e., 10×3 beams, we achieve the required $\Delta T = 0.3$ K—indeed an ambitious option.

If we under-illuminate the reflector to achieve the required FP = 5 km we calculate properties as found using a 3.8 m aperture: 5 km FP, $\Delta T = 1.43$ K, 90 RPM. Now, we need eight beams along track, and will thus achieve $\Delta T = 0.51$ K. One extra row of beams, i.e., 8×2 beams will provide $\Delta T = 0.36$ K, which is probably acceptable.

The L-band channel will, using the 5 m aperture, have an FP of 99 km, which will have to be accepted for this secondary channel. The radiometric resolution will be $\Delta T = 0.15$ K, so only one beam provides a satisfactory result.

C. Conclusion

In summary, the baseline option fulfilling requirements calls for a 5-m aperture and:

- 1) 1 beam @ L-band, $\Delta T = 0.15$ K;
- 2) 2 beams along track @ C-band, $\Delta T = 0.15$ K;
- 3) 3 beams along track, 2 beams across track (6 beams) @ X-band, $\Delta T = 0.29$ K;
- 4) 5 beams along track, 2 beams across track (10 beams) @ Ku-band, $\Delta T = 0.33$ K;
- 5) 8 beams along track, 2 beams across track (16 beams) @ Ka-band, $\Delta T = 0.36$ K;
- 6) 11.3 RPM antenna rotation rate;
- 7) fore or aft look;
- 8) swath (using $\pm 60^\circ$ scan): 1524 km.

If we use the full-resolution potential of the 5-m aperture at Ka-band, we must use:

- 1) 10 beams along track, 3 beams across track (30 beams) @ Ka-band, $\Delta T = 0.30$ K

III. FROM TRADITIONAL FEED HORN TO FPA

Many beams make it impractical to consider traditional feed horns due to congestion in the feed area. The cross-polarization purity requirement and the distance-to-coast requirement (see Section I) translate into the need for a very fine antenna beam with low side-lobes and high beam efficiency—very difficult to achieve with a traditional feed horn [5].

Instead, a dense array of a large number of smaller antenna elements can be used, and by summing the outputs from

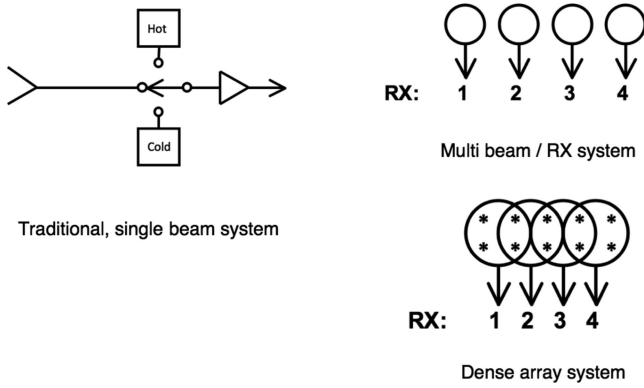


Fig. 3. From traditional horn to dense array system.

clusters of those, adjusted properly in phase and amplitude, beams having the desired properties can be generated.

This dense array approach has been successfully implemented in several designs of high-sensitivity receivers for radio astronomy [9], and this work was partly inspired by these designs. Fig. 3 illustrates the concept: to the left is shown a traditional setup where one antenna horn is connected to a radiometer receiver. When several beams are needed, individual horns may be connected to equally many receivers, as shown top right, but this may lead to congestion in the horn area. Bottom right shows the system in which 4 beams are created from 10 small elements (*) and connected to 4 receivers. Also, it shows how the signal from one element contributes to more than one beam.

Generally, many elements are needed—it could be 30 H-polarized and 30 V-polarized elements—to build one beam. As already stated, the outputs of the elements are summed, properly adjusted in amplitude and phase, to make a beam. The V-polarized beam primarily consists of contributions from the V-polarized elements, but small contributions from the H-polarized elements are added to obtain a final beam with very low cross polarization. Also, this method of creating the beam by contributions from many small elements enables an almost perfect beam with very low side-lobes. This may pave the way for accurate ocean measurements very close to coastlines (and sea ice). Finally, it is noticeable that it is possible to make more than one beam using the same elements. Two beams are thus readily possible. Several beams require more elements in the FPA, but the number of elements does not increase proportionally with the number of beams, as it does when using traditional feed horns.

In Section IV, a system is discussed where 2 beams at L-band require 32 dual-polarized elements, and 2 beams at C-band can also be achieved using slightly more than 30 dual-polarized elements. In [2] and [10], systems having up to 30 beams are discussed. Thirty beams typically require 140–160 dual-polarized elements. More details can be found in [5].

IV. DESIGN EXAMPLE: A NEW C-& L-BAND SYSTEM WITH FPA FEED

The issues discussed earlier, as well as the consequences for receiver design and resource demands, will be evaluated by

TABLE IV
INSTRUMENT SPECIFICATIONS

Frequency (GHz)	BW (MHz)	Polarization	ΔT (K)	FP (km)	Dist. to coast (km)
6.9	300	H & V St. 3 & 4	0.18 0.25	20	15-20
1.4	19	H & V St. 3 & 4	0.10 0.14	100	50-100

means of a design example based on the TWIST instrument originally proposed as a candidate for ESA's Earth Explorer 9, and on the ongoing work on a next-generation large scanning system named Copernicus Imaging Microwave Radiometer (CIMR) [11]. The baseline requirements for the instrument are measurements of brightness temperatures at frequencies near 7 GHz with a radiometric resolution around 0.2 K and with a spatial resolution on ground around 20 km. In addition, measurements using the same antenna aperture at 1.4 GHz with a radiometric resolution around 0.10 K are required. A maximum antenna rotation rate of 12 RPM is required. An altitude of 817 km and an incidence angle of 53° on ground are assumed. A summary of the specifications for the instrument, as provided by the customer/funding agency, is shown in Table IV.

A. Radiometric Resolution

A conically scanning system is evaluated concerning the antenna size, spatial resolution, radiometric resolution, coverage, and antenna rotation rate, just as described in Section II.

The bandwidth at C-band is 300 MHz, and the noise figure is 1.4 dB corresponding to $T_N = 110$ K. The parameters at L-band are 19 MHz and 76 K.

The antenna *beam* is assumed to look at a calm sea surface at V polarization. Hence, the brightness temperatures can be calculated using Klein & Swift, resulting in $T_A = 155$ K at C-band and 145 K at L-band. Thus, the system noise is $T_{SYS} = T_A + T_N = 265$ K at C-band and 221 K at L-band.

The result for the instrument is that a 5-m aperture leads to the required 20 km FP at C-band. A 5-m aperture leads to a 99 km FP at L-band.

The C-band channel will have ΔT around 0.21 K for the normal channels and 0.30 K for Stokes 3 and 4, and the antenna will rotate with 22.6 RPM. Neither the radiometric sensitivity nor the rotation rate is acceptable. Two beams along track and 2 associated receiver systems will result in $\Delta T = 0.15$ K and 11.3 RPM rotation. The third and the fourth Stokes parameters will have $\Delta T = 0.21$ K.

The L-band channel will have an FP of 99 km, and a $\Delta T = 0.14$ K. The specifications call for 0.10 K. As already explained, we can implement several beams along track and achieve better sensitivity. We can also implement several beams across track such that a point on ground is measured several times with a short time interval. Integrating over these independent measurements results in better sensitivity. Two simultaneous beams across track and the associated receiver systems yield $\Delta T = 0.10$ K. However, there is a cost issue: more beams typically

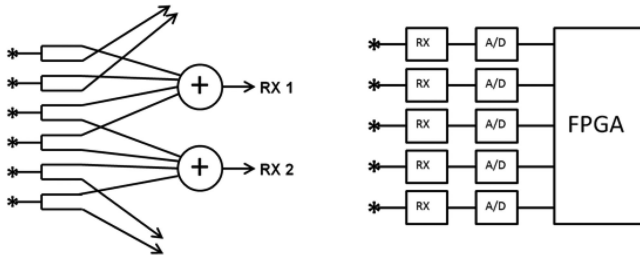


Fig. 4. FPA receiver system.

means more antenna feed horns and more receivers. Thus, there will be a discussion between engineering, customer, and user community. In some cases, requirements are relaxed and the one-beam solution accepted in order to reduce cost. Here, this is not an issue since we use an FPA, and two beams are readily provided without extra feed elements or receivers.

It should be noted that the earlier discussion assumes that the instrument only have one look toward the ground: fore or aft. In this polarimetric system, we cannot consider the possibility to integrate fore and aft looks in order to improve ΔT by sqrt. 2. Thus, we must stick to one look: fore or aft.

It must also be noted that more beams along track might be a favorable option even if not required due to radiometric resolution: it leads to lower antenna rotation rate, which can be a very important issue for the mechanical system design and cost.

In summary, the baseline option adequately fulfilling requirements calls for:

- 1) 2 beams along track @ 6.9 GHz, $\Delta T = 0.15$ K;
- 2) 2 beam @ 1.4 GHz, $\Delta T = 0.10$ K;
- 3) 11.3 RPM;
- 4) fore or aft look.

B. FPA/Beams/RX Issues

The receiver system configuration and resource demands—especially concerning power consumption—are discussed and evaluated in the following, using existing state-of-the-art components. These are important issues in the present context: it is of little practical interest that excellent beam performance can be achieved if the receiving system becomes impractical and very power consuming.

The antenna is based on a feed system where a dense array of a large number of small antenna elements is used, and by summing the outputs from clusters of those elements, adjusted properly in phase and amplitude, the individual beams are generated. Fig. 4 (left) illustrates in a classical way the concept, where signals from different elements (*) are added and fed into a receiver to create one beam. Each element contributes to more than one beam.

However, it is impossible to apply power splitters and combining network directly after the elements from a noise point of view, so each element must be connected to its own receiver, followed by A/D conversion [see Fig. 4 (right)]. The beam forming then takes place in a Field-Programmable Gate Array (FPGA), using complex digital multipliers and adders.

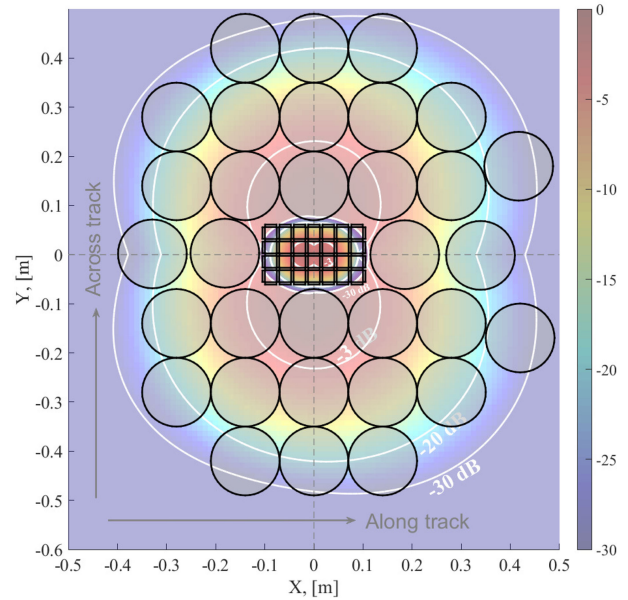
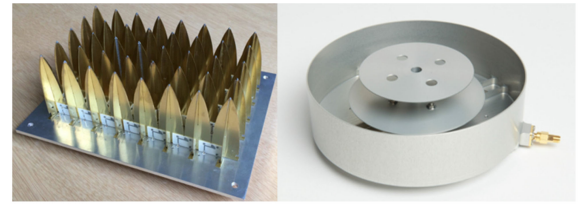


Fig. 5. Vivaldi array and patch-excited cup antenna element (top) and layout of the antenna arrays in the reflector focal plane (bottom). The focal field distribution, when -30 dB tapered plane waves are incident on the reflector from directions of the beams, is shown as background image.

For the present design example, a $4 \times 8 + 5 \times 7 = 67$ element Vivaldi antenna array was chosen for C-band and a breadboard was designed and built in order to investigate modeling of a broad-bandwidth antenna element [12] (see Fig. 5). For L-bands, an existing dual-polarized and space-proven patch/cup antenna element was chosen [13]. Fig. 5 (bottom) also shows how the 32 dual-polarized L-band elements can be fitted around the Vivaldi array.

The design of the L-band and C-band arrays consists of two steps: 1) determining the maximum acceptable distance between antenna elements for the proper focal field sampling; and 2) finding the focal plane area which should be filled with the antenna elements, which determines size of the array.

According to the Nyquist sampling criteria, the distance between the antenna elements d should be less than half wavelengths of the focal field distribution. However, a slight increase of d may lead to acceptable radiometric performance degradation. This issue was studied in detail in [14], and it was concluded that the element separation of $0.7\text{--}0.75\lambda$ is sufficient from the radiometric performance point of view but will lead to significant reduction of the antenna elements in the array.

The element separation $d = 0.67\lambda$ @ 6.9 GHz was chosen from the feeding (reflection coefficient) perspective of the Vivaldi elements at C-band, and the physical size of the patch antennas at L-band ($140\text{ mm} \Leftrightarrow d \approx 0.66\lambda$ @ 1.4 GHz).

TABLE V
SIMULATED RADIOMETRIC CHARACTERISTICS

Radiometer characteristic	L-band		C-band	
	Beam 1	Beam 2	Beam 1	Beam 2
Distance to land, [km]	89.9	87.7	13.5	14.6
Rel. cross-pol. power, [%]	0.25	0.15	0.17	0.18
Beam efficiency*, [%]	97.6	97.7	97.3	97.4
Average footprint, [km]	91.1	91.1	19.0	19.0
Footprint ellipticity	1.44	1.44	1.75	1.76

* The beam efficiency is defined here at -20 dB level.

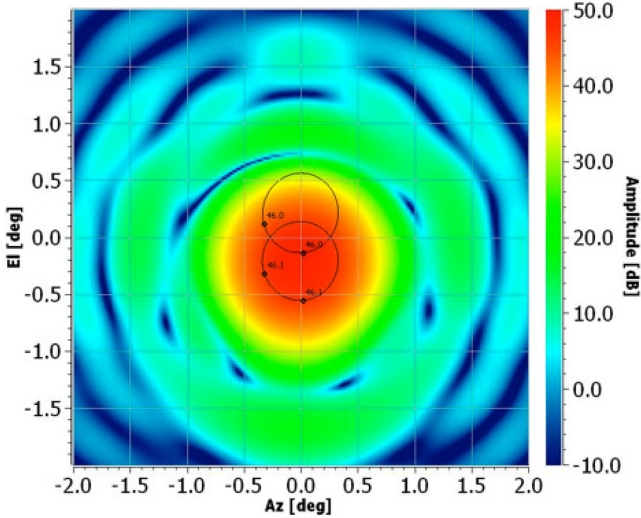


Fig. 6. C-band FPA makes two beams with suitable overlap.

The number of elements and the layout of the arrays are determined by the focal field amplitude distribution when tapered plane waves are incident on the reflector from the directions of all desired beams (see Fig. 5). The antenna elements should cover an area with the field amplitude down to -20 , \dots , -30 dB, from its maximum. The taper of the plane waves is selected to be -30 dB at the reflector edge, which leads to a good first-order approximation of the actual focal field distribution when the arrays are excited with the optimal weight coefficients. For more information on the radiometer performance when Conjugate Field Matching beamformer is used with different taper of the incident plane wave, refer to [15].

Once the array layout is fixed, the resulting beam can be formed using an optimization process that determines the elements excitation amplitudes and phases. In this study, we used the beamforming algorithm described in [16], which is based on the conventional maximum signal-to-noise ratio beamformer. Another beamforming algorithm [5] gives very similar radiometric performance. In the present case, the performance fulfills all the requirements (see Table V).

Fig. 6 illustrates the performance of one C-band beam (in color code), including a lineout of the -3 dB FP. A second along-track beam is also shown using a lineout of its -3 dB FP. A suitable overlap of 30% has been used in order to ensure proper sampling of the brightness temperature scenario. The requirements state a max. 0.34% cross-polarization contamination. Analysis of these beams shows that we can achieve 0.15%

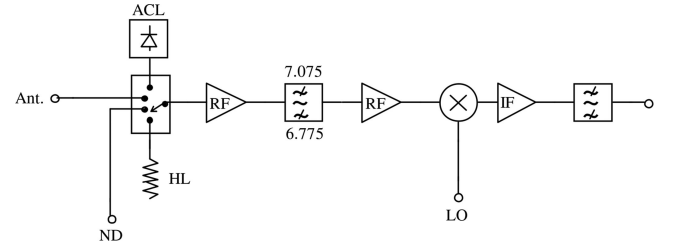


Fig. 7. C-band receiver.

corresponding to a 0.1 K error, as well as 99.7% of the power within a cone angle of 0.8° such that the 15 km distance to coast requirement is fulfilled [17].

C. Calibration Issues

It is of little interest to design a radiometer system with a fancy antenna system if it is difficult to calibrate. Traditionally, scanners are calibrated while the antenna beam looks away from the swath: a mirror diverts the beam toward free space on one side, and the feeds are covered by a microwave load on the other side (see [6]). In the present design example, this method is still feasible at C-band, but looking at Fig. 5, it seems like the L-band system is so large that this will be a challenge.

However, calibration can also be done satisfactorily internally by using matched loads, noise injection signals, and active cold loads (ACLs). SMOS, which is a salinity mission with very stringent calibration requirements, relies on such internal calibration (no ACLs) being done frequently and supported by observation of the sky from time to time to fix the absolute level (see [18]). Internal calibration is assumed in the current design example.

D. Receiver Design and Power Consumption

Receivers can be designed using the direct or the superheterodyne method. The direct layout can, in principle, serve L- and C-bands using advanced but present-day A/D converter technology. But fast converters require much power. The superheterodyne layout means more analog components, especially including a mixer and a local oscillator (LO), but a suitable IF frequency relaxes the A/D converter demands.

Fig. 7 illustrates a straightforward implementation of a receiver system able to handle the C-band. The L-band receiver has the same layout.

The input switch can select a noise signal (ND), common to all receivers. This signal is primarily to validate the coherence between channels but can also be used for calibration. Hot or cold calibration points (a matched load and an ACL) can also be selected by the switch. The switch must be of low loss. A low-noise amplifier without too much gain (enough to overcome subsequent filter loss, but limited in order not to saturate due to RFI signals in the broad input band) supplies the filters and the mixer generating the IF signal suitable for A/D conversion.

The following component types have been addressed: switch; low-noise amplifier; mixer; LO; IF amplifier; and especially A/D converter. No specific research has been carried out for space

qualified components, or fancy new laboratory developments—just small, low-noise commercial components.

Relevant components are listed as follows:

- 1) Input switch (MA4AGSW4): L- through Ka-bands, 0.4–1.0 dB loss, very little power;
- 2) Mixer: powered by LO;
- 3) Oscillator: 300 mW;
- 4) IF amplifier: GALI-S66, 20 dB gain, 60 mW power;
- 5) C-band amplifier: CGY2120, 0.6 dB NF, 13 dB gain, 50 mW power;
- 6) L-band amplifier: MAAL-011078, 0.4 dB NF, 24 dB gain, 90 mW power.

The gains of these amplifiers are such that the C-band receiver needs 4 RF amps and 2 IF amps in series, and the L-band receiver needs 2 RF amps plus 3 IF amps in series. In addition, each receiver needs 1 RF amp used as ACL.

All the components considered here are small chip-like units well suited for very compact monolithic microwave integrated circuit (MMIC) designs. Thus, bulk and weight is no issue.

A realistic power budget for one C-band receiver can now be established, and the result is 370 mW per receiver. Our system has 67 C-band receivers, so the total power for the C-band receivers is 25 W.

The L-band receiver is treated the same way, and a realistic power budget for one L-band receiver is 450 mW. Our system has 64 L-band receivers, so the total power for the L-band receivers is 29 W.

Concerning the LO system, we need 10 mW per mixer. We have $67 + 64 = 131$ mixers, i.e., $0.01 \times 131 = 1.3$ W. The signals for the mixers are generated in two oscillators, each 300 mW, followed by amplification. Assuming an amplifier efficiency of 50%, the total power for the LO circuitry is 3 W.

The noise injection calibration circuitry contributes by an insignificant amount.

The beamforming network is based on the powerful Zynq UltraScale+ RFSoc FPGA that includes 16 each 2 GSPS 12-bit A/D converters. Analog bandwidth is 4 GHz, and the estimated power consumption is ≈ 20 W.

Since there are 16 A/D converters in one FPGA, it would be very attractive if 64 C-band receivers could do the job adequately. The performance of the system has been re-evaluated omitting the 4 corner elements in the FPA, and by proper tuning, indeed practically the same performance can be achieved (the corner elements already had a very low weighting).

Thus, the C-band system at first glance requires 4 FPGAs each consuming about 20 W.

However, this is far from using the full potential of the FPGA and the potential of its A/D converters. First, investigations have shown that FPGA is very large compared with the requirements of the VHDL code performing the beam forming. Second, the receiver bandwidth is only 300 MHz while the A/D converters can operate with 2 GSPS. We have receivers for H and V polarizations. The LO frequency for the H channel can be set to 6.675 GHz and the LO for V to 6.275 GHz. The two IF outputs are added and fed into one A/D converter. Frequencies are 100–400 and 500–800 MHz. Later in the system, the two channels are separated again digitally. A sampling frequency of 1.7 GHz

is assumed. Thus, the C-band system requires only two FPGAs, each consuming about 20 W; so the total power for the C-band A/D conversion and beam forming circuitry is 40 W.

L-bands, having much lower bandwidths, can easily be treated the same way, but still two FPGAs are deemed necessary in order to handle the beamforming properly. Thus, the total power for the L-band A/D conversion and beam forming circuitry is 40 W.

Thus, the current estimate for the power consumption of the receivers, LOs, calibration, and beamforming, is 137 W.

This power consumption is more than typically experienced for a traditional radiometer system but much less than seen for many other remote sensing systems such as radar systems. Thus, it is considered acceptable, and a system could be designed and built for installation in a typical spacecraft platform.

V. SUMMARY

A spaceborne imaging microwave radiometer system, having a hitherto unseen performance, has been designed and evaluated, and it is a candidate for a next-generation ocean mission. The instrument focuses on C-band, which is important for the SST, wind vector measurements, and sea ice parameters. The instrument is designed to fly behind MetOpSG, and the Microwave Imager will thus provide the necessary data at higher frequencies. This means that we can use a large mesh reflector antenna that can be folded for launch (similar to SMAP). The baseline design uses a 5-m aperture providing a 20 km -3 dB FP on the ocean surface.

The instrument is augmented by an L-band channel, thus providing sea surface salinity (SSS) and thin sea ice measurements at 100 km -3 dB FP.

Land/sea contamination (and sea-ice/sea contamination) has been a challenge ever since the start of microwave radiometry from space. The problem is the large brightness temperature contrast when passing over the coast (or ice) line in combination with realistic antenna patterns. No matter how well you design the feed horn, it is just not good enough when considering this issue. The problem can be solved by using an FPA as feed: many small feed elements (around 30 per polarization) illuminate the reflector, and by properly adding the output of each element in amplitude and phase, an almost perfect antenna beam can be generated. The challenge is that where a traditional system would have a single radiometer receiver per polarization, the FPA-based system will, for each polarization, have 30 receivers, 30 fast A/D converters (the full RF bandwidth must be digitized), as well as significant and fast digital processing hardware—all onboard and in real time. However, we note that technology has developed such that this is now realistic.

Radiometric sensitivity also becomes an issue in high-spatial resolution, wide-swath imagers. By using two simultaneous beams at each frequency and the latest technology, $\Delta T = 0.2$ K can be achieved at C-band and 0.10 K at L-band.

We note that the FPA can produce two beams without any resource costs.

The new instrument, having a 5-m antenna rotating with 12 RPM, will from an 817-km orbit measure a 1524 km swath at 53° incidence angle, thus providing a frequent coverage of the

Earth (especially in ice-infested Arctic regions). The C-band channel at 6.9 GHz will measure all four Stokes parameters with $\Delta T = 0.15$ K (0.21 K for Stokes 3 and 4) and will provide meaningful measurements of the ocean as close to coast (and sea ice) as 15–20 km. This is substantially better than anything seen hitherto! Also, cross-polarization issues are handled by the FPA concept, and the instrument will provide unsurpassed V- and H-polarization purity.

Using off-the-shelf commercial low-power components, the power consumption for the basic receiver and processing units is calculated to 137 W.

The instrument will provide unique all-weather SST globally, also in cloudy areas like near equator and far north/south, as well as wind vectors under severe weather conditions. The measurements will have excellent quality even very close to coasts and sea ice edges.

ACKNOWLEDGMENT

RUAG Space, Sweden, designed the L-band cup antenna and provided the simulation data.

REFERENCES

- [1] D. Stammer, J. Johannesssen, P.-Y. LeTraon, P. Minnett, H. Roquet, and M. Srokosz, "Requirements for ocean observations relevant to post-EPS," in *Proc. AEG Ocean Topography Ocean Imaging*, Jan. 2007, p. 40.
- [2] TICRA, DTU-Space, Chalmers, HPS, "Final report, study on advanced multiple-beam radiometers," ESTEC Contract No. 4000107369/12/NL/MH, 2014.
- [3] The Advanced Microwave Scanning Radiometer—Earth Observing System (AMSR-E). 2019. [Online]. Available: <http://nsidc.org/data/NSIDC-0301>. Accessed on: Nov. 15, 2017.
- [4] P. W. Gaiser, "The WindSat spaceborne polarimetric microwave radiometer: Sensor description and early orbit performance," *IEEE Trans. Geosci. Remote Sens.*, vol. 42, no. 11, pp. 2347–2361, Nov. 2004.
- [5] O. A. Iupikov, M. V. Ivashina, N. Skou, C. Cappellin, K. Pontoppidan, and K. van 't Klooster, "Multi-beam focal plane arrays with digital beamforming for high precision space-borne ocean remote sensing," *IEEE Trans. Antennas Propag.*, vol. 66, no. 2, pp. 737–748, Feb. 2018.
- [6] N. Skou and D. Le Vine, *Microwave Radiometer Systems: Design & Analysis*, 2nd ed. Norwood, MA, USA: Artech House, 2006, p. 222.
- [7] L. Klein and C. Swift, "An improved model for the dielectric constant of sea water at microwave frequencies," *IEEE Trans. Antennas Propag.*, vol. 25, no. 1, pp. 104–111, Jan. 1977.
- [8] J. R. Piepmeyer *et al.*, "SMAP L-band microwave radiometer: Instrument design and first year on orbit," *IEEE Trans. Geosci. Remote Sens.*, vol. 55, no. 4, pp. 1954–1966, Apr. 2017.
- [9] K. F. Warnick, R. Maaskant, M. V. Ivashina, D. Bruce Davidson, and B. D. Jeffs, "High-sensitivity phased array receivers for radio astronomy," *Proc. IEEE*, vol. 104, no. 3, pp. 607–622, Mar. 2016.
- [10] N. Skou *et al.*, "Future spaceborne ocean missions using high sensitivity multiple-beam radiometers," in *Proc. IGARSS 2014*, Jul. 2014, pp. 2546–2549.
- [11] 2019. [Online]. Available: www.cimr.eu
- [12] C. Cappellin *et al.*, "Feed array breadboard for future passive microwave radiometer antennas," in *Proc. 12th Eur. Conf. Antennas Propag.*, London, U.K., 2018, pp. 1–5.
- [13] J. Johansson and P. Ingvarsson, "Array antenna activities at RUAG space. An overview," in *Proc. Eur. Conf. Antennas Propag.*, Gothenburg, Sweden, Apr. 2013, pp. 666–669.
- [14] O. A. Iupikov *et al.*, "Dense focal plane arrays for pushbroom satellite radiometers," in *Proc. 8th Eur. Conf. Antennas Propag.*, The Hague, The Netherlands, Apr. 2014, pp. 3536–3540.
- [15] C. Cappellin *et al.*, "Novel multi-beam radiometers for accurate ocean surveillance," in *Proc. 8th Eur. Conf. Antennas Propag.*, The Hague, The Netherlands, Apr. 2014, pp. 3531–3535.
- [16] O. A. Iupikov *et al.*, "An optimal beamforming algorithm for phased-array antennas used in multi-beam spaceborne radiometers," in *Proc. Eur. Conf. Antennas Propag.*, Lisbon, Portugal, Apr. 2015, pp. 1–5.
- [17] J. R. de Lasson *et al.*, "Innovative multi-feed-per-beam reflector antenna for space-borne conical-scan radiometers," in *Proc. AP-S/URSI Conf.*, Boston, MA, USA, Jul. 2018, pp. 1729–1730.
- [18] M. Marti'n-Neira *et al.*, "SMOS instrument performance and calibration after six years in orbit," *Remote Sensing Environ.*, vol. 180, pp. 19–39, Feb. 2016.



Niels Skou (S'78–M'79–SM'96–F'03) received the M.Sc., Ph.D., and D.Sc. degrees from the Technical University of Denmark, Kongens Lyngby, Denmark, in 1972, 1981, and 1990, respectively.

His research has been directed toward microwave remote sensing systems. After working for three years with the development of radar systems for measuring the ice sheets in Greenland and Antarctica, his interest turned toward microwave radiometry. He developed a scanning, multifrequency, airborne radiometer system. After that, his subjects were radiometer measurements of sea ice and oil pollution on the sea, spaceborne radiometer systems, and development of new systems for specific purposes. In the mid-1980s, his interest turned back to active instruments, and he became involved in the development of an airborne, multifrequency, polarimetric, and interferometric synthetic aperture radar system, with special emphasis on calibration fidelity. However, activity within microwave radiometry has continued, mainly within the areas of synthetic aperture radiometry and polarimetric radiometry. The work on synthetic aperture radiometry has led to the European Space Agency's Soil Moisture and Ocean Salinity (SMOS) Mission, and he was a member of the SMOS Science Advisory Group. In support of SMOS, a range of airborne campaigns with L-band radiometers have been carried out over land, sea, the Arctic sea ice, and the East Antarctica Dome-C. He has taken a special interest in radio frequency interference (RFI), using digital signal processing and polarimetry to detect and mitigate harmful RFI. He is currently a Professor Emeritus with the Technical University of Denmark. He is also a member of the SMOS Quality Working Group. His current research interests include development of a real-time RFI processors and the design of very small receiver systems for focal plane arrays, both to be used in the next generation of spaceborne radiometers.



Sten Schmidl Søjbjerg (M'99) received the M.Sc.E.E. and Ph.D. degrees from the Technical University of Denmark (DTU), Kongens Lyngby, Denmark, in 1996 and 2003, respectively.

He is currently an Associate Professor at the Microwave Remote Sensing Section, DTU-Space Department, DTU. He participated in the development of an airborne fully polarimetric dual frequency scanning radiometer system for 16 and 34 GHz in order to determine the wind direction over the ocean. From 2001, he has been involved in working with the EMIRAD L-band polarimetric radiometer featuring advanced digital detection. He has participated in several airborne campaigns for preparation, calibration, and validation for the ESA/Soil Moisture and Ocean Salinity (SMOS) mission. His current research interests include accurate instrument calibration and data quality assessment, including detection and mitigation of RF interference. His current research interests include polarimetric microwave radiometers and their applications, with focus on instrumentation and measurement campaigns.



Steen Savstrup Kristensen (M'17) received the M.Sc.E.E. degree from the Technical University of Denmark (DTU), Kongens Lyngby, Denmark, in 1985.

He is currently with the DTU, where he has been participating in designing and operating both radars and radiometers. He has been the Mission Manager for several campaigns such as ice-sounder campaigns in Greenland, the POLARIS data acquisition during the IceGrav-2011 campaign in Antarctica and the EMIRAD data acquisition during the SMOSIce-2013

campaign in Antarctica. Programming and managing the off-line processing facilities for several sensors such as EMIRAD, EMISAR, and Ice-sounders has also been part of his activities. Recently, he has been involved in developing, designing, and implementing online RFI mitigation techniques for a radiometer system for MetOp Second Generation and implementing online processing for the Atmosphere Space Interaction Monitor mounted on the International Space Station in 2018. His current research interests include microwave remote sensing systems.



Cecilia Cappellin (M'08) received the M.Sc. degree in telecommunication engineering from the University of Siena, Siena, Italy, in 2004, and the industrial Ph.D. degree from the Technical University of Denmark (DTU), Kongens Lyngby, Denmark, in 2007.

In her Ph.D., she developed an antenna diagnostics technique for spherical near-field antenna measurements. In 2004, she joined TICRA, Copenhagen, Denmark, where she is currently the Head of the Applied Electromagnetics Team (AEM Team) and Product Lead of the Reflector Systems Designs. As

Product Lead, she is responsible for TICRA's analysis and design of reflector antenna systems. As a member of the AEM team, she actively participates in the test and development cycles of all TICRA software products and assists TICRA's customers under their technical support contract. She has been leading numerous ESA projects. She is currently engaged in the ESA/EU activities on large mesh reflectors and in ESA studies on advanced multibeam radiometers.



Knud Pontoppidan received the M.Sc.E.E. and Ph.D. degrees from the Technical University of Denmark (DTU), Kongens Lyngby, Denmark, in 1965 and 1972, respectively.

He joined TICRA, Copenhagen, Denmark, in 1972. Since then, he has been engaged in radio telescopes, deployable reflector antennas and contoured beam antennas, omnidirectional or near-anisotropic antennas, physical optics and the geometrical theory of diffraction. He has by now 45 years of experience in reflector antenna analysis and design. A large effort

has been devoted to the influence of reflector tolerances and reflector electrical properties. He has been a Project Manager and Technical responsible of uncountable ESA contracts and antenna designs. He has also been engaged in the design and analysis of compact test ranges. Within this field, he has especially investigated the coupling between the range and the antenna under test. He has been the initiator of a study on reconfigurable reflectors made by piano wires net, investigating the mechanical, electrical, and mathematical properties of the reconfigurable net. He has developed significant parts of the GRASP software, and he is among the best experts of the software, providing continuous support to TICRA's customers on all TICRA's software packages (GRASP, POS, and CHAMP).



Jakob Rosenkrantz de Lasson received the M.Sc.Eng. degree in physics and nanotechnology and the Ph.D. degree in nanophotonics from the Technical University of Denmark (DTU), Kongens Lyngby, Denmark, in 2012 and 2015, respectively.

The main topics of his Ph.D. degree were periodic and photonic bandgap media (photonic crystals), slow light, coupled cavity-waveguide structures, and plasmonic nanostructures. In 2016, he joined the Applied Electromagnetics Team, TICRA, where he is working on R&D and analysis and design of antennas for space applications. He has worked on several ESA projects, including activities on large deployable reflector antennas as well as focal plane arrays and microwave radiometers for future Earth observation missions. In addition, he is TICRA's Product Lead for Mission Planning and Analysis.



Marianna V. Ivashina (M'11–SM'13) received the Ph.D. degree in electrical engineering from Sevastopol National Technical University (SNTU), Sevastopol, Ukraine, in 2001.

From 2001 to 2010, she was with The Netherlands Institute for Radio Astronomy (ASTRON), where she carried out research on innovative phased-array technologies for future radio telescopes, such as the Square Kilometer Array (SKA). She is currently a Professor of Antenna Systems at Chalmers University of Technology, Gothenburg, Sweden. She has authored or coauthored extensively on the earlier topics, having authored/coauthored over 120 journal and conference papers. Her current research interests include wideband receiving arrays, antenna system modeling techniques, receiver noise characterization, signal processing for phased arrays, and radio astronomy.

Dr. Ivashina is currently an Associate Editor of the IEEE TRANSACTIONS ON ANTENNAS AND PROPAGATION.



Oleg A. Iupikov (M'16) received the M.Sc. degree in electrical engineering from the Sevastopol National Technical University (SNTU), Sevastopol, Ukraine, in 2006, and the Ph.D. degree from the Chalmers University of Technology, Gothenburg, Sweden, in 2017.

After graduating, he was at the Radio Engineering Bureau, Sevastopol. During this period, he was also a Visiting Researcher at The Netherlands Institute for Radio Astronomy (ASTRON), where he was involved in the development of the focal plane array simulation software for the APERTIF radio telescope. He is currently a Post-doctoral Researcher with the Chalmers University of Technology. His current research interests include receiving antenna array systems, in particular focal plane arrays for radio astronomy and microwave remote sensing applications, numerical methods for their analysis and optimization, signal processing algorithms for antenna systems, and integration of antennas with active components.